



Chaetomugilins I–O, new potent cytotoxic metabolites from a marine-fish-derived *Chaetomium* species. Stereochemistry and biological activities

Yasuhide Muroga, Takeshi Yamada*, Atsushi Numata, Reiko Tanaka

Osaka University of Pharmaceutical Sciences, 4-20-1 Nasahara, Takatsuki, Osaka 569-1094, Japan

ARTICLE INFO

Article history:

Received 16 March 2009

Received in revised form 29 June 2009

Accepted 29 June 2009

Available online 4 July 2009

Keywords:

Chaetomugilin

Chaetomium globosum

Growth inhibition

Marine fish

CD spectrum

Absolute stereostructure

COMPARE program

ABSTRACT

Chaetomugilins I–O were isolated from a strain of *Chaetomium globosum* originally isolated from the marine fish *Mugil cephalus*, and their absolute stereostructures were elucidated on the basis of spectroscopic analyses, including 1D and 2D NMR techniques, as well as chemical transformations. These compounds exhibited significant growth inhibition of cultured P388, HL-60, L1210, and KB cell lines. In addition, chaetomugilin I showed selective cytotoxic activity against 39 human cancer cell lines.

© 2009 Elsevier Ltd. All rights reserved.

1. Introduction

Marine microorganisms are potentially prolific sources of highly bioactive secondary metabolites that might serve as useful leads in the development of new pharmaceutical agents. Based on the fact that some of the bioactive materials isolated from marine animals have been produced by bacteria, we have focused our attention on new antitumor agents from microorganisms separated from marine organisms.^{1–6} As part of this endeavor, we have reported that cytotoxic azaphilones, chaetomugilins A–H, were produced by *Chaetomium globosum* strain OUPS-T106B-6, which was originally isolated from the marine fish *Mugil cephalus*.^{7,8} Research of diverse secondary metabolites through the OSMAC (one strain, many compounds) approach has led to the discovery of concise methods to analyze the structures of natural products. Our continuing search for cytotoxic metabolites from this fungal strain has led to the isolation of seven new azaphilones designated as chaetomugilins I–O (1–7). Azaphilones have various bioactivities, including antimicrobial activity, nitric oxide inhibitory activity (cohaerins),⁹ gp120-CD4 binding inhibitory activity (isochromophilones, ochreophilone, scretotiorin, and rubrorotiorin),¹⁰ monoamine oxidase inhibitory activity (luteusins, TL-1, TL-2, and chaetoviridins),^{11,12} platelet-derived growth factor binding inhibitory activity (RP-1551s),¹³ and antimalarial activity (cochliodones).¹⁴ The

metabolites isolated in this investigation exhibited significant cytotoxic activity against the murine P388 leukemia cell line, the human HL-60 leukemia cell line, the murine L1210 leukemia cell line, and the human KB epidermoid carcinoma cell line. In addition, chaetomugilin I (1) was proved to show selective cytotoxicity to a disease-oriented panel of 39 human cancer cell lines. We describe herein the absolute stereostructures and biological activities of these compounds.

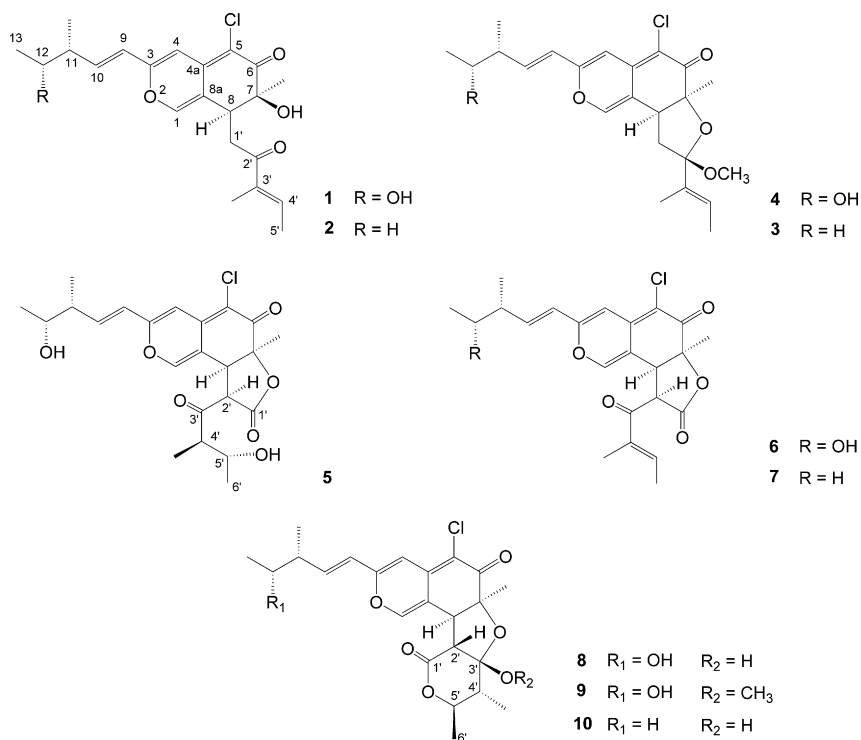
2. Results and discussion

The microorganism from *M. cephalus* fish was cultured at 27 °C for 6 weeks in a medium (50 L) containing 1% soluble starch and 0.1% casein in 50% artificial seawater adjusted to pH 7.4, as reported previously.^{7,8} After incubation, the AcOEt extract of the culture filtrate was purified by bioassay-directed fractionation (cytotoxicities to the P388 cell line) employing a stepwise combination of Sephadex LH-20 chromatography, silica gel column chromatography, and reversed-phase HPLC to afford chaetomugilins I–O (1–7).

Chaetomugilin I (1) had the molecular formula C₂₂H₂₇ClO₅ as established by the [M+H]⁺ peak in high-resolution fast atom bombardment mass spectrometry (HRFABMS) and the ratio of isotope peak intensities (MH⁺/[MH+2]⁺). Its IR spectrum exhibited bands at 3442, 1639, and 1617 cm⁻¹, which are characteristic of hydroxyl and α,β -unsaturated carbonyl groups. Close inspection of the ¹H and ¹³C NMR spectra (Table 1) of 1 by DEPT and HMQC experiments revealed the presence of two secondary methyls (11-CH₃

* Corresponding author. Tel.: +81 72 690 1085; fax: +81 72 690 1084.

E-mail address: yamada@gly.oups.ac.jp (T. Yamada).



and C-13), one tertiary methyl (7-CH₃), one secondary olefin methyl (C-5'), one tertiary olefin methyl (3'-CH₃), one sp³-hybridized methylene (C-1'), three sp³-methines (C-8, C-11, and C-12) including one oxygen-bearing carbon (C-12), five sp²-methines (C-1, C-4, C-9, C-10, and C-4') including one oxygen-bearing carbon (C-1), one quaternary oxygen-bearing sp³-carbon (C-7), five

quaternary sp²-carbons (C-3, C-4a, C-5, C-8a, and C-3') including one oxygen-bearing carbon (C-3), and two carbonyls (C-6 and C-2'). ¹H-¹H COSY analysis of **1** yielded three partial structural units, as shown by boldface lines in Figure 1. The geometrical configuration of the double bond moiety (C-9-C-10) was deduced to be trans from the coupling constant of the olefinic protons (*J*_{9,10}=16.0 Hz).

Table 1
NMR spectral data of **1–4** in CDCl₃

Position	1			2			3			4		
	$\delta_{\text{H}}^{\text{a}}$	<i>J</i> /Hz	δ_{C}	$\delta_{\text{H}}^{\text{a}}$	<i>J</i> /Hz	δ_{C}	$\delta_{\text{H}}^{\text{a}}$	<i>J</i> /Hz	δ_{C}	$\delta_{\text{H}}^{\text{a}}$	<i>J</i> /Hz	δ_{C}
1	7.48 s		145.66 (d)	7.47 s		145.72 (d)	7.06 s		142.74 (d)	7.06 s		140.66 (d)
3			156.65 (s)			157.17 (s)			156.42 (s)			155.88 (s)
4	6.47 s		104.99 (d)	6.45 s		104.51 (d)	6.45 s		104.70 (d)	6.48 s		105.28 (d)
4a			141.56 (s)			141.79 (s)			138.73 (s)			138.47 (s)
5			106.78 (s)			106.47 (s)			111.17 (s)			111.56 (s)
6			191.89 (s)			191.82 (s)			188.84 (s)			188.88 (s)
7			74.08 (s)			74.07 (s)			83.78 (s)			83.77 (s)
8	3.48 dd	10.5 (1'A), 3.0 (1'B)	40.51 (d)	3.48 dd	10.2 (1'A), 2.2 (1'B)	40.51 (d)	2.93 t	7.8 (1'A, 1'B)	43.79 (d)	2.93 t	7.8 (1'A, 1'B)	43.80 (d)
8a			119.49 (s)			119.50 (s)			117.04 (s)			117.11 (s)
9	6.12 d	16.0 (10)	122.26 (d)	6.02 d	15.5 (10)	120.35 (d)	6.02 d	15.5 (10)	120.56 (d)	6.12 d	15.5 (10)	122.52 (d)
10	6.58 dd	16.0 (9), 7.2 (11)	141.85 (d)	6.48 dd	15.5 (9), 6.5 (11)	146.12 (d)	6.42 dd	15.5 (9), 7.9 (11)	145.00 (d)	6.53 dd	15.5 (9), 8.1 (11)	142.65 (d)
11	2.44 sex	7.2 (10, 12, 11-CH ₃)	44.16 (d)	2.24 sept	6.5 (10, 12, 11-CH ₃)	38.79 (d)	2.24 m		38.69 (d)	2.44 m		44.07 (d)
12	3.80 quint	7.2 (11,13)	70.81 (d)	1.42 qd	7.5 (13), 6.5 (11)	29.16 (t)	1.42 m		29.23 (t)	3.81 quint	6.5 (11, 13)	70.94 (d)
13	1.19 d	6.5 (12)	20.37 (q)	0.89 t	7.5 (12)	11.67 (q)	0.90 t	7.5 (12)	11.68 (q)	1.19 d	6.5 (12)	20.40 (q)
7-CH ₃	1.33 s		26.74 (q)	1.33 s		26.79 (q)	1.40 s		23.59 (q)	1.40 s		23.58 (q)
11-CH ₃	1.12 d	7.2 (11)	14.80 (q)	1.07 d	6.5 (11)	19.38 (q)	1.07 d	6.5 (11)	19.41 (q)	1.12 d	7.1 (11)	14.77 (q)
1'A	2.62 dd	17.5 (1'B), 10.5 (8)	34.80 (t)	2.62 dd	17.3 (1'B), 10.2 (8)	34.86 (t)	2.14 dd	13.6 (1'B), 7.8 (8)	45.67 (t)	2.14 dd	13.0 (1'B), 7.8 (8)	45.69 (t)
1'B	3.27 dd	17.5 (1'A), 3.0 (8)		3.28 dd	17.3 (1'A), 2.2 (8)		2.35 dd	13.6 (1'A), 7.8 (8)	45.67 (t)	2.35 dd	13.0 (1'A), 7.8 (8)	45.69 (t)
2'			199.38 (s)			199.41 (s)			108.52 (s)			108.52 (s)
3'			137.97 (s)						133.56 (s)			133.53 (s)
4'	6.66 q	7.5 (5')	137.97 (d)	6.66 q	7.1 (5')	137.96 (d)	5.94 q	6.8 (5')	122.47 (d)	5.94 q	6.8 (5')	122.49 (d)
5'	1.81 d	7.5 (4')	14.68 (q)	1.80 d	7.1 (4')	14.69 (q)	1.65 d	6.8 (4')	13.12 (q)	1.65 d	6.8 (4')	13.12 (q)
3'-CH ₃	1.73 s		10.49 (q)	1.73 s		10.99 (q)	1.56 s		12.29 (q)	1.57 s		12.29 (q)
2'-OCH ₃							3.05 s		49.43 (q)	3.05 s		49.42 (q)

^a ¹H chemical shift values (δ ppm from SiMe₄) followed by multiplicity and then the coupling constants (*J*/Hz). Figures in parentheses indicate the proton coupling with that position.

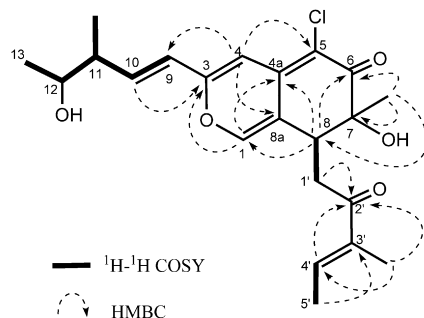
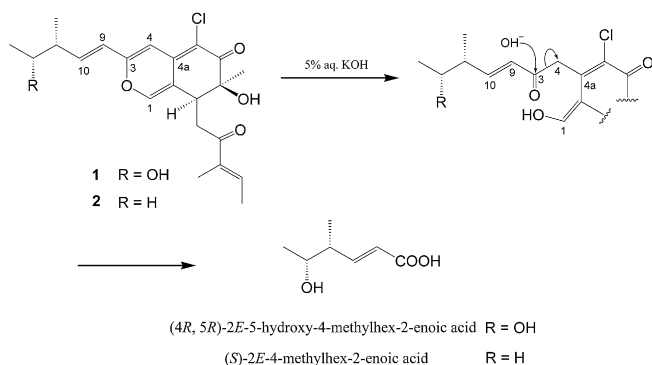


Figure 1. ^1H - ^1H COSY and key HMBC correlations in **1**.

The connections of these units and the remaining functional groups were determined on the basis of key HMBC data summarized in Figure 1. The connection of a chlorine atom to C-5 was reasonable from the molecular formula. In addition, the double bond moiety (C-3'-C-4') was deduced to have an *E* configuration from the NOE correlations (H-4'/H-1'A and H-4'/H-1'B). Thus, the planar structure of **1** was elucidated, as shown in Figure 1. In order to determine the absolute configuration at C-11 and C-12, alkaline degradation of **1** was carried out. The degradation of **1** with 5% potassium hydroxide afforded a carboxylic acid that was identified as (4*R*,5*R*)-2*E*-5-hydroxy-4-methylhex-2-enoic acid, which was obtained from chaetomugilin A (**8**) in a similar manner (Scheme 1). This carboxylic acid was considered to be a new compound in terms of stereochemistry. Thus, the absolute configuration at C-11 and C-12 of **1** was established as *R* and *R*, respectively.



Scheme 1. Plausible mechanism for alkaline degradation of **1** and **2**.

Chaetomugilin J (**2**) ($\text{C}_{22}\text{H}_{27}\text{ClO}_4$) had one oxygen atom less than **1**, as deduced from HRFABMS. The general features of its UV, IR, and NMR spectra (Table 1) closely resembled those of **1** except for the NMR signals of the side chain moiety (C-9–C-13) [proton signals: H-9 (δ_{H} 6.02, d), H-10 (δ_{H} 6.48, dd), H-11 (δ_{H} 2.24, sept), H-12 (δ_{H} 1.42, qd), H-13 (δ_{H} 0.89, t), and 11- CH_3 (δ_{H} 1.07, d); carbon signals: C-9 (δ_{C} 120.35), C-10 (δ_{C} 146.12), C-11 (δ_{C} 38.79), C-12 (δ_{C} 29.16), C-13 (δ_{C} 11.67), and 11- CH_3 (δ_{C} 19.38)]. These data implied that the hydroxyl methine at C-12 in **1** was replaced with a methylene in **2**. The planar structure of **2** was confirmed by ^1H - ^1H COSY and HMBC experiments. Subjecting **2** to the same alkaline degradation as **1** gave (*S*)-2*E*-4-methylhex-2-enoic acid, which was identified by comparison with a commercial sample¹⁵ (Scheme 1). The absolute stereochemistry at C-7 and C-8 of **1** and **2** was established by derivation from chaetomugilin K (**4**) and chaetomugilin L (**3**), respectively, as described later.

Chaetomugilin L (**3**), $\text{C}_{23}\text{H}_{29}\text{ClO}_4$, showed spectral features closely resembling those of **2** except for a methoxy group that appeared newly and the replacement of the conjugated carbonyl (C-2') in **2** with a ketal [δ_{C} 108.52 (C-2'); δ_{H} 2.14, 2.35 (H-1'); δ_{C} 45.67 (C-1') ppm] (Table 1). The planar structure of **3** was confirmed by analyzing HMBC connectivities (from the methoxy group to C-2';

from H-4' to C-2' and C-3'; from 3'- CH_3 to C-2'; and from H-5' to C-3'). The above lines of evidence and the ^{13}C NMR chemical shift of C-7 (δ_{C} 83.78), together with the molecular formula of **3**, suggested the presence of an ether linkage between C-7 and C-2'. In the NOESY experiment of **3**, the observed NOEs (Fig. 2) implied that H-8 is oriented *cis* to 7- CH_3 and *trans* to 2'- OCH_3 , and that the double bond moiety (C-3'-C-4') has an *E* configuration. Whalley et al. have shown that the sign of the specific rotation of azaphilones is apparently controlled by the absolute configuration at C-7.¹⁶ Steyn and Vleggaar established the absolute stereochemistry of azaphilones from the definition of the absolute configuration at C-7 of (+)-sclerotiorin in the CD spectra. In addition, they revealed that the Cotton curve remained unaffected by the functional groups at C-8.¹⁷ In the CD spectrum of chaetomugilin B (**9**) (Fig. 3),⁷ the absolute stereostructure of which was established by X-ray analysis, the Cotton curve ($\Delta\epsilon_{323} -4.2$) clearly showed the *S*-configuration at C-7. Based on this evidence, the absolute configuration at C-7 of **3** was determined to be *S*, because its CD spectrum showed a negative Cotton effect ($\Delta\epsilon_{323} -4.9$) (Fig. 3). Treatment of **3** in MeOH with 0.5 N HCl gave product **2** (yield 84.2%), which was confirmed to be identical with natural **2** in terms of IR, UV, and NMR spectra as well as optical rotation. The results revealed that the absolute configuration at C-11 of **3** is *S*. In addition, the absolute configuration at C-7 and C-8 of **2**, which has hitherto remained undecided, was established as *S* and *S*, respectively. The CD curve ($\Delta\epsilon_{322} -3.9$) of **2** supported that the absolute configuration at C-7 of **2** was *S*.

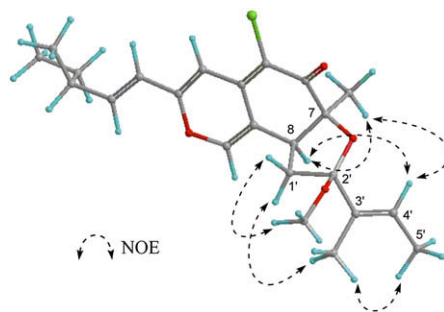


Figure 2. Observed NOEs in **3**.

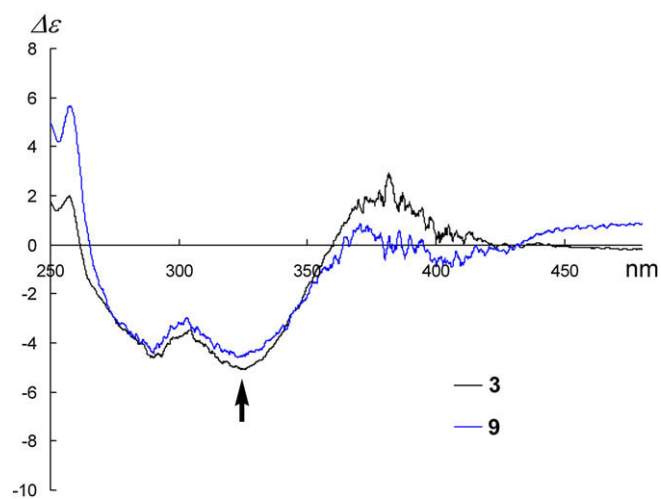


Figure 3. CD spectra of **3** and **9**.

Chaetomugilin K (**4**), $\text{C}_{23}\text{H}_{29}\text{ClO}_5$, had one more oxygen atom than **3**. Its spectral data were similar to those of **3**, except for the presence of a hydroxyl group at C-12, which was revealed by the IR absorption band at 3448 cm^{-1} and the comparison of its NMR spectra for the side chain moiety with those of **1**. The absolute

Table 2
NMR spectral data of **5–7** in CDCl₃

Position	5			6			7		
	$\delta_{\text{H}}^{\text{a}}$	J/Hz	δ_{C}	$\delta_{\text{H}}^{\text{a}}$	J/Hz	δ_{C}	$\delta_{\text{H}}^{\text{a}}$	J/Hz	δ_{C}
1	7.40 s		146.24 (d)	7.32 s		145.76 (d)	7.33 s		145.81 (d)
3			157.27 (s)			157.25 (s)			157.73 (s)
4	6.51 s		105.17 (d)	6.52 s		105.13 (d)	6.49 s		104.63 (d)
4a			140.72 (s)			140.39 (s)			140.54 (s)
5			109.56 (s)			109.84 (s)			109.56 (s)
6			184.45 (s)			184.76 (s)			184.68 (s)
7			83.44 (s)			83.46 (s)			83.47 (s)
8	3.90 d	12.1 (2')	42.47 (d)	4.12 d	12.5 (2')	43.43 (d)	4.11 d	12.0 (2')	43.42 (d)
8a			113.63 (s)			113.69 (s)			113.66 (s)
9	6.13 d	15.9 (10)	122.07 (d)	6.13 d	15.8 (10)	121.99 (d)	6.04 d	15.7 (10)	120.10 (d)
10	6.62 dd	15.9 (9), 7.8 (11)	142.62 (d)	6.61 dd	15.8 (9), 7.8 (11)	142.75 (d)	6.50 dd	15.7 (9), 7.0 (11)	146.97 (d)
11	2.46 m		44.06 (d)	2.45 dqd	7.8 (10), 6.5 (11-CH ₃), 5.5 (12)	44.14 (d)	2.25 sept	7.0 (10, 12, 11-CH ₃)	38.85 (d)
12	3.83 m		70.81 (d)	3.81 qd	6.2 (13), 5.5 (11)	70.79 (d)	1.41 m		29.12 (t)
13	1.19 d	6.2 (12)	20.27 (q)	1.18 d	6.2 (12)	20.35 (q)	0.89 t	7.0 (12)	11.67 (q)
7-CH ₃	1.61 s		23.47 (q)	1.63 s		23.21 (q)	1.63 s		23.22 (q)
11-CH ₃	1.12 d	6.9 (11)	14.61 (q)	1.12 d	6.5 (11)	14.72 (q)	1.07 d	7.0 (11)	19.34 (q)
1'			168.85 (s)			168.34 (s)			168.33 (s)
2'	4.23 d	12.1 (8)	58.74 (d)	4.38 d	12.5 (8)	51.56 (d)	4.37 d	12.0 (8)	51.59 (d)
3'			207.02 (s)			191.38 (s)			191.39 (s)
4'	3.20 dq	9.1 (5'), 6.6 (4'-CH ₃)	52.76 (d)			137.51 (s)			137.5 (s)
5'	3.80 m		72.62 (d)	6.81 q	7.0 (6')	144.77 (d)	6.80 q	7.0 (6')	144.73 (d)
6'	1.24 d	5.9 (5')	22.34 (q)	1.94 d	7.0 (5')	15.40 (q)	1.94 d	7.0 (5')	15.40 (q)
4'-CH ₃	1.06 d	6.6 (4')	13.00 (q)	1.84 s		11.27 (q)	1.84 s		11.27 (q)

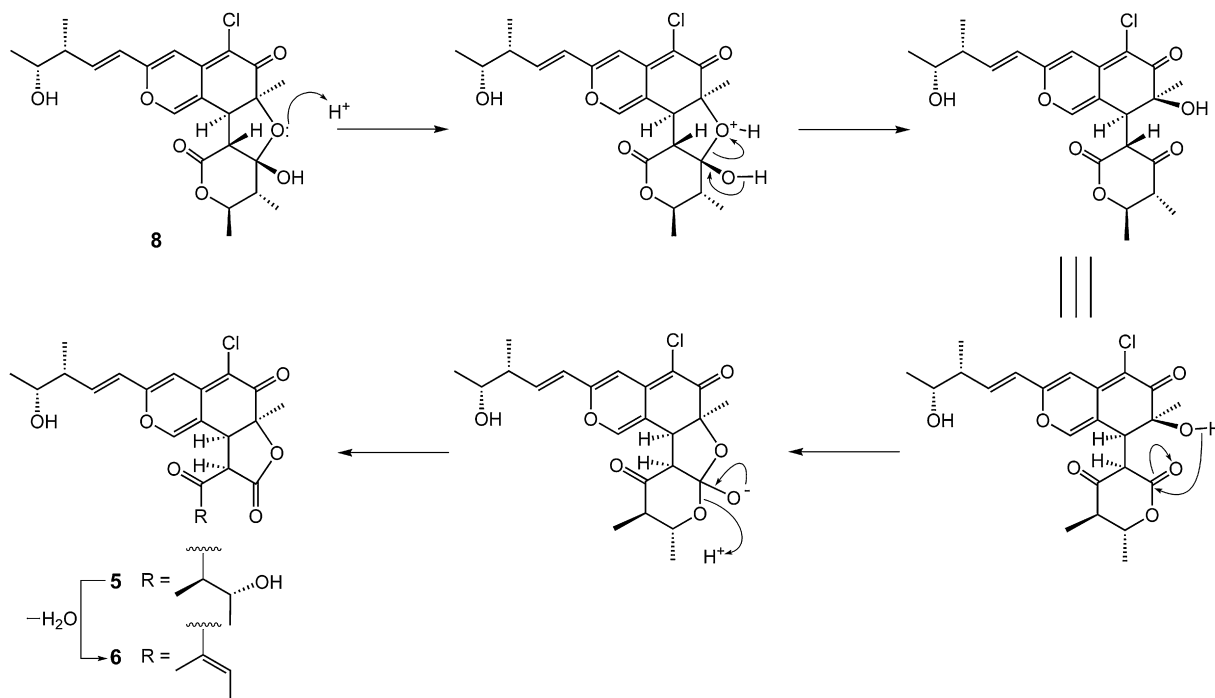
^a As in Table 1.

configuration at C-7 of **4** was also determined to be *S* based on the CD spectrum that showed a positive Cotton effect ($\Delta\epsilon_{321} -4.0$). This result allowed us to assign the absolute configuration at all the asymmetric centers (7*S*, 8*S*, and 2'*S*) except C-11 and C-12. Furthermore, the transformation of **4** into **1** by the above reaction that formed **2** from **3** gave product **1** (yield 59.1%), which was confirmed to be identical with natural **1** in terms of spectral data and specific optical rotation. Thus, the results confirmed the absolute stereostructures of chaetomugilin I (**1**) (11*R*, 12*R*, 7*S*, and 8*S*) and chaetomugilin K (**4**) (11*R*, 12*R*, 7*S*, 8*S*, and 2'*S*).

In the process of isolation, the culture filtrate was extracted with AcOEt, and the time that **1** and **2** were exposed to MeOH on LH-20 and the silica gel column chromatography was very short (6–7 h, the longest time). In addition, compounds **1** and **2** were stable in

MeOH for a few days. Therefore, the above results support the assumption that both **3** and **4** were not artifacts of these compounds.

Chaetomugilin M (**5**) was assigned the molecular formula C₂₃H₂₇ClO₇ based on deductions made from HRFABMS data. Its IR spectrum showed an absorption band characteristic of a γ -lactone (1779 cm⁻¹). The ¹H and ¹³C NMR spectra (Table 2) of **5** were typical of the above azaphilone skeleton (C-1–C-13), and analyses of HMBC correlations (from H-8 to C-3'; from H-2' to C-1'; and from 4'-CH₃ to C-3') confirmed that **5** had a planar structure. As the stereochemistry of **5** could not be deduced from NOESY experiments, the derivation of **5** from chaetomugilin A (**8**)⁷ was attempted (Scheme 2). Treatment with *p*-TsoH of **8** in MeOH gave two minor products **5** and chaetomugilin N (**6**) as described later (yields 1.5% and 0.7%, respectively). As shown in a previous report, this reaction formed



Scheme 2. Plausible mechanism for transformation of chaetomugilin A (**8**) into **5** and **6**.

other chaetomugilins as major products⁷ and therefore, the yields of reaction products **5** and **6** were very low. The reaction mechanism summarized in Scheme 2 revealed the absolute stereostructures of chaetomugilins M (**5**) and N (**6**), as will be described later.

Chaetomugilin N (**6**), C₂₃H₂₅ClO₆, had one oxygen atom and two hydrogen atoms less than **5**. Its spectral data were similar to those of **5** except for the olefin carbon signals that were observed newly in the ¹³C NMR spectrum and the 2D NMR experiments of **6**, indicating the presence of a double bond conjugating with the carbonyl (C-3') at C-4'-C-5' (Table 2). The absolute stereostructure of **6** was established by derivation from chaetomugilin A (**8**),⁷ as described above (Scheme 2). In addition, treatment of **5** with *p*-TsOH also gave **6** (Scheme 2). This fact implied that the transformation of **8** into **6** proceeded through **5**.

Chaetomugilin O (**7**), C₂₃H₂₅ClO₅, had one oxygen atom less than **6**. Its ¹H and ¹³C NMR spectra (Table 2) were notably different from those of **6**, namely, the spectra showed signals for the side chain moiety, and **7** was confirmed to be 12-dehydroxy chaetomugilin N by 2D NMR spectral analyses and comparison with the data for the side chain moiety of chaetomugilins J (**2**) and L (**3**). The chemical transformation of chaetomugilin D (**10**)⁸ gave two products: chaetoviridin C¹² and **7** (yields 1.9% and 0.4%, respectively), and revealed the absolute stereostructure of **7**.

As a primary screen for antitumor activity, cancer cell growth inhibitory properties of new chaetomugilins **1–7** were examined using the murine P388 leukemia cell line, the human HL-60 leukemia cell line, the murine L1210 leukemia cell line, and the human KB epidermoid carcinoma cell line. All compounds except **5** exhibited significant cytotoxic activity against the cancer cell lines (Table 3). **1** in particular showed more potent cytotoxic activity against human cancer cell lines (HL-60 and KB cells) than 5-FU, the positive control. In addition, **1** was examined using a disease-oriented panel of 39 human cell lines.^{18,19} As shown in Table 4, the effective concentration (MG-MID), the delta value, and the range value of **1** revealed that **1** had potent and selective cytotoxic activity (effective value: MG-MID < -5, delta ≥ 0.5, and range ≥ 1.0). Furthermore, evaluation of the pattern of differential cytotoxicity using the COMPARE program^{18,19} suggested that the mode of action of **1** might be different from that shown by any other anticancer drugs developed to date.

Table 3
Cytotoxicity of the metabolites against P388, HL-60, L1210 and KB cell lines

Compounds	Cell line P388	Cell line HL-60	Cell line L1210	Cell line KB
	IC ₅₀ (mM) ^a	IC ₅₀ (mM) ^a	IC ₅₀ (mM) ^a	IC ₅₀ (mM) ^a
Chaetomugilin 1 (1)	1.1	1.1	1.9	2.3
2 (2)	12.6	12.6	2.8	8.5
4 (4)	8.2	14.1	11.2	18.7
3 (3)	10.9	13.1	15.6	20.1
5 (5)	>100	>100	>100	>100
6 (6)	2.3	2.3	10.6	10.6
7 (7)	11.1	11.1	10.1	7.2
5-FU ^b	1.7	2.7	1.1	7.7

^a DMSO was used for vehicle.

^b Positive control.

3. Experimental

3.1. General

Mps were determined on a Yanagimoto micro-melting point apparatus and are uncorrected. UV spectra were recorded on a Hitachi U-2000 spectrophotometer and IR spectra, on a JASCO FT/IR-680 plus. NMR spectra were recorded at 27 °C on Varian UNITY INOVA-500 and MERCURY spectrometers with tetramethylsilane (TMS) as internal reference. FABMS was determined using a JEOL JMS-700 (Ver. 2) mass spectrometer. Optical rotations were recorded on a JASCO J-820 polarimeter. Liquid chromatography over silica gel

Table 4
Cytotoxicity of chaetomugilin **1** against a panel of 39 human cancer cell lines

Origin of cancer	Cell line	log GI50 ^a	Origin of cancer	Cell line	log GI50 ^a
Breast	HBC-4	-5.07	Melanoma	LOX-IMVI	-5.26
	BSY-1	-5.50		Ovary	OVCAR-3
	HBC-5	-5.25	OVCAR-4		-5.48
	MCF-7	-4.98	OVCAR-5		-5.36
	MDA-MB-231	-5.38	OVCAR-8		-4.84
Central nervous system	U-251	-4.94	Kidney	SK-OV-3	-4.57
	SF-268	-4.97		RXF-631L	-4.63
	SF-295	-4.81		ACHN	-5.51
	SF-539	-5.42	Stomach	St-4	-4.85
	SNB-75	-5.42		MKN1	-5.70
	SNB-78	-5.17		MKN7	-5.44
Colon	HCC2998	-4.88	Prostate	MKN28	-5.12
	KM-12	-5.09		MKN45	-4.71
	HT-29	-5.32		MKN74	-4.79
	HCT-15	-5.32		DU-145	-4.79
	HCT-116	-5.42	PC-3	-5.52	
	Lung	NCI-H23	-4.87	MG-MID ^b	
NCI-H226		-4.94	Delta ^c		0.63
NCI-H522		-5.78	Range ^d		1.21
NCI-H460		-4.76			
A549		-4.68			
DMS273		-5.32			
DMS114		-5.32			

^a log concentration of compounds for inhibition of cell growth at 50% compared to control.

^b Mean value of log GI50 over all cell lines tested.

^c The difference in log GI50 value of the most sensitive cell and MG-MID value.

^d The difference in log GI50 value of the most sensitive cell and the least sensitive cell.

(mesh 230–400) was performed at medium pressure. HPLC was run on a Waters ALC-200 instrument equipped with a differential refractometer (R 401) and Shim-pack PREP-ODS (25 cm × 20 mm i. d.). Analytical TLC was performed on precoated Merck aluminum sheets (DC-Alufolien Kieselgel 60 F₂₅₄, 0.2 mm) with the solvent system CH₂Cl₂–MeOH (19:1), and compounds were viewed under a UV lamp and sprayed with 10% H₂SO₄, followed by heating.

3.2. Culture and isolation of metabolites

A strain of *C. globosum* was initially isolated from the marine fish *M. cephalus* collected in Katsura Bay in Japan in October 2000. The fish was wiped with EtOH and its gastrointestinal tract applied to the surface of nutrient agar layered in a Petri dish. Serial transfers of one of the resulting colonies yielded a pure strain of *C. globosum*. The fungal strain was cultured at 27 °C for six weeks in a liquid medium (50 L) containing soluble starch 1% and casein 0.1% in 50% artificial seawater adjusted to pH 7.4. The culture was filtered under suction and the mycelia collected were extracted thrice with MeOH. The combined extracts were evaporated in vacuo to give a mixture of crude metabolites (23.8 g), the CHCl₃–MeOH (1:1) soluble fraction of which exhibited cytotoxicity. The culture filtrate was extracted thrice with AcOEt. The combined extracts were evaporated in vacuo to afford a mixture of crude metabolites (20.3 g) that exhibited cytotoxicity (ED₅₀ 35.8 μg/mL). The AcOEt extract was passed through Sephadex LH-20 using CHCl₃–MeOH (1:1) as the eluent. The second fraction (7.2 g) in which the activity was concentrated was chromatographed on a silica gel column with a CHCl₃–MeOH gradient as the eluent. The CHCl₃ eluate (720.5 mg) was purified by HPLC using MeCN–H₂O (80:20) as the eluent to afford chaetomugilin D (**10**, 121.3 mg), Fr. 1 (45.2 mg), chaetomugilin F (22.2 mg), chaetomugilin E (24.1 mg), chaetomugilin O (**7**, 6.1 mg), chaetomugilin J (**2**, 7.7 mg), and chaetomugilin L (**3**, 7.6 mg). Fr. 1 was purified by HPLC using MeCN–H₂O (60:40) as eluent to afford chaetomugilin H (10.5 mg). The MeOH–CHCl₃ (1:99) eluate

(489.3 mg) was purified by HPLC using MeOH–H₂O (50:50) as the eluent to afford chaetomugilin I (**1**, 15.7 mg) and chaetomugilin K (**4**, 14.1 mg). The MeOH–CHCl₃ (1:99) eluate (1.8 g) was purified by HPLC using MeOH–H₂O (50:50) as the eluent to afford chaetomugilin A (**8**, 143.2 mg), chaetomugilin M (**5**, 22.3 mg), Fr.2 (79.5 mg), chaetomugilin C (44.1 mg), chaetomugilin B (**9**, 38.5 mg), and chaetomugilin N (**6**, 8.5 mg). Fr. 2 was purified by HPLC using MeCN–H₂O (35:65) as eluent to afford chaetomugilin G (17.2 mg).

3.2.1. Chaetomugilin I (**1**)

Yellow powder; mp 98–100 °C (CHCl₃–MeOH); [α]_D +210.2 (c 0.04, EtOH); UV λ_{\max} (EtOH)/nm (log ϵ): 291 (3.27), 385 (3.75), 405 (3.59); IR ν_{\max} (KBr)/cm⁻¹: 3442, 1639, 1617, 1561, 1523; HRFABMS m/z 407.1618 [M+H]⁺ (calcd for C₂₂H₂₈³⁵ClO₅: 407.1625). ¹H and ¹³C NMR data are listed in Table 1.

3.2.2. Chaetomugilin J (**2**)

Yellow powder; mp 99–101 °C (CHCl₃–MeOH); [α]_D +243.8 (c 0.10, EtOH); UV λ_{\max} (EtOH)/nm (log ϵ): 290 (3.81), 374 (3.84), 405 (3.91); IR ν_{\max} (KBr)/cm⁻¹: 3448, 1651, 1620, 1560, 1520; HRFABMS m/z 391.1673 [M+H]⁺ (calcd for C₂₂H₂₈³⁵ClO₄: 391.1676). ¹H and ¹³C NMR data are listed in Table 1.

3.2.3. Chaetomugilin L (**3**)

Yellow powder; mp 152–154 °C (CHCl₃–MeOH); [α]_D –319.3 (c 0.09, EtOH); UV λ_{\max} (EtOH)/nm (log ϵ): 290 (3.81), 375 (3.86), 405 (3.92); IR ν_{\max} (KBr)/cm⁻¹: 1649, 1568, 1523; HRFABMS m/z 404.1757 [M]⁺ (calcd for C₂₃H₂₉³⁵ClO₄: 404.1755). ¹H and ¹³C NMR data are listed in Table 1.

3.2.4. Chaetomugilin K (**4**)

Yellow powder; mp 222–224 °C (CHCl₃–MeOH); [α]_D –65.7 (c 0.14, EtOH); UV λ_{\max} (EtOH)/nm (log ϵ): 291 (3.75), 373 (3.73), 410 (3.80); IR ν_{\max} (KBr)/cm⁻¹: 3448, 1621, 1559, 1523; HRFABMS m/z 420.1694 [M]⁺ (calcd for C₂₃H₂₉³⁵ClO₅: 420.1703). ¹H and ¹³C NMR data are listed in Table 1.

3.2.5. Chaetomugilin M (**5**)

Yellow powder; mp 119–121 °C (CHCl₃–MeOH); [α]_D –103.8 (c 0.12, EtOH); UV λ_{\max} (EtOH)/nm (log ϵ): 292 (3.75), 374 (3.75), 413 (3.82); IR ν_{\max} (KBr)/cm⁻¹: 3431, 1779, 1643, 1563, 1515; HRFABMS m/z 451.1521 [M+H]⁺ (calcd for C₂₃H₂₈³⁵ClO₇: 451.1524). ¹H and ¹³C NMR data are listed in Table 2.

3.2.6. Chaetomugilin N (**6**)

Yellow powder; mp 127–129 °C (CHCl₃–MeOH); [α]_D –71.8 (c 0.14, EtOH); UV λ_{\max} (EtOH)/nm (log ϵ): 292 (3.74), 380 (3.69), 419 (3.80); IR ν_{\max} (KBr)/cm⁻¹: 3448, 1781, 1642, 1563, 1522; HRFABMS m/z 433.1419 [M+H]⁺ (calcd for C₂₃H₂₆³⁵ClO₆: 433.1418). ¹H and ¹³C NMR data are listed in Table 2.

3.2.7. Chaetomugilin O (**7**)

Yellow powder; mp 95–97 °C (CHCl₃–MeOH); [α]_D –116.1 (c 0.14, EtOH); UV λ_{\max} (EtOH)/nm (log ϵ): 292 (3.72), 372 (3.72), 412 (3.80); IR ν_{\max} (KBr)/cm⁻¹: 1781, 1642, 1563, 1522; HRFABMS m/z 417.1466 [M+H]⁺ (calcd for C₂₃H₂₆³⁵ClO₅: 417.1468). ¹H and ¹³C NMR data are listed in Table 2.

3.3. Degradation

3.3.1. Degradation of **1** by potassium hydroxide

Chaetomugilin I (**1**) (20.2 mg) was dissolved in 10 mL of 5% aq potassium hydroxide and the reaction mixture was stirred for 3 h at 100 °C. Then, the reaction mixture was extracted with 10 mL of CHCl₃. The water layer was adjusted to pH 3.0 with 9% sulfuric acid and re-extracted with 10 mL of AcOEt. The organic extract

was concentrated to dryness in vacuo. The residue was purified by HPLC using MeCN–H₂O gradient (0:100 to 60:40) as the eluent to afford (4*R*,5*R*,2*E*)-5-hydroxy-4-methylhex-2-enoic acid (0.9 mg). Using the same procedure, chaetomugilin A (56.8 mg), the absolute stereostructure of which was determined already, was treated with 5% aq potassium hydroxide (20 mL) and purified by HPLC to afford (4*R*,5*R*)-2*E*-5-hydroxy-4-methylhex-2-enoic acid (3.1 mg).

3.3.1.1. (4*R*,5*R*)-2*E*-5-Hydroxy-4-methylhex-2-enoic acid. Colorless oil; [α]_D +90.0 (c 0.05, EtOH); HRFABMS m/z :145.0867 [M+H]⁺ (calcd for C₇H₁₃O₃: 145.0865); ¹H NMR δ ppm (CDCl₃): 1.12 (3H, d, J =6.5 Hz, 4-CH₃), 1.19 (3H, d, J =6.2 Hz, H-6), 2.44 (1H, dqd, J =7.5, 6.5, 6.2 Hz, H-4), 3.80 (1H, quint, J =6.2 Hz, H-5), 5.90 (1H, d, J =15.5 Hz, H-2), 7.06 (1H, d, J =15.5, 7.5 Hz, H-3).

3.3.2. Degradation of **2** by potassium hydroxide

Chaetomugilin J (**2**) (15.5 mg) was dissolved in 15 mL of 5% aq potassium hydroxide and the reaction mixture was stirred for 3 h at 100 °C. Then, the reaction mixture was extracted with 15 mL of CHCl₃. The water layer was adjusted to pH 3.0 with 9% sulfuric acid and re-extracted with 15 mL of petroleum ether. The organic extract was concentrated to dryness in vacuo. The residue was purified by HPLC using MeCN–H₂O gradient (0:100 to 100:0) as the eluent to afford (*S*)-2*E*-4-methylhex-2-enoic acid (0.5 mg). The physicochemical properties of this carboxylic acid were identical with those of a commercial sample.¹⁵

3.4. Derivatization

3.4.1. Transformation of **3** into **2**

One drop of 0.5 N HCl aq was added to a MeOH solution (1 mL) of chaetomugilin L (**3**) (4.8 mg), and the reaction mixture was left to stand at room temperature for 3 h. The solvent was evaporated off under reduced pressure and the residue was purified by HPLC using MeCN–H₂O (80:20) as the eluent to afford **2** (3.9 mg).

3.4.2. Transformation of **4** into **1**

Using the same procedure as that for **3**, chaetomugilin K (**4**) (5.6 mg) was treated with 0.5 N HCl aq (1 drop) in MeOH (1 mL) and the products were purified by HPLC using MeCN–H₂O (50:50) as the eluent to afford **1** (3.2 mg).

3.4.3. Transformation of chaetomugilin A (**8**) into **5** and **6**

p-TsOH (8.5 mg) was added to a MeOH solution (1 mL) of **8** (80.1 mg) and the reaction mixture was left to stand at room temperature for 3 h. The solvent was evaporated off under reduced pressure and the residue was purified by HPLC using MeCN–H₂O (35:65) as the eluent to afford **5** (1.2 mg) and **6** (0.5 mg).

3.4.4. Transformation of **5** into **6**

Using the same procedure as above for **8**, chaetomugilin M (**5**) (8.2 mg) was treated with *p*-TsOH (1.1 mg) in MeOH (1 mL) and the products were purified by HPLC using MeCN–H₂O (50:50) as the eluent to afford **6** (0.7 mg).

3.4.5. Transformation of chaetomugilin D (**10**) into chaetoviridin C and **7**

Using the same procedure as above for **8**, **10** (79.8 mg) was treated with *p*-TsOH (7.5 mg) in MeOH (1 mL) and the products were purified by HPLC using MeCN–H₂O (80:20) as the eluent to afford chaetoviridin C (1.5 mg) and **7** (0.3 mg).

3.4.6. Transformation of chaetoviridin C into **7**

Using the same procedure as above for **8**, chaetoviridin C (20.2 mg) was treated with *p*-TsOH (1.9 mg) in MeOH (1 mL) and

the products were purified by HPLC using MeCN–H₂O (80:20) as the eluent to afford **7** (2.6 mg).

3.5. Assay for cytotoxicity

Cytotoxic activities of chaetomugilins I–O (**1–7**) were examined with the 3-(4,5-dimethyl-2-thiazolyl)-2,5-diphenyl-2H-tetrazolium bromide (MTT) method. P388, HL-60, L1210, and KB cells were cultured in Eagle's Minimum Essential Medium (10% fetal calf serum) at 37 °C in 5% CO₂. The test material was dissolved in dimethyl sulfoxide (DMSO) to give a concentration of 10 mM, and the solution was diluted with the Essential Medium to yield concentrations of 200, 20, and 2 μM, respectively. Each solution was combined with each cell suspension (1×10⁵ cells/mL) in the medium, respectively. After incubating at 37 °C for 72 h in 5% CO₂, grown cells were labeled with 5 mg/mL MTT in phosphate buffered saline (PBS), and the absorbance of formazan dissolved in 20% sodium dodecyl sulfate (SDS) in 0.1 N HCl was measured at 540 nm with a microplate reader (Model 450, BIO-RAD). Each absorbance value was expressed as percentage relative to that of the control cell suspension that was prepared without the test substance using the same procedure as that described above. All assays were performed three times, semi-logarithmic plots were constructed from the averaged data, and the effective dose of the substance required to inhibit cell growth by 50% (IC₅₀) was determined.

Acknowledgements

We thank Dr. T. Yamori (Screening Committee of Anticancer Drugs supported by a Grant-in-Aid for Scientific Research on Priority Area 'Cancer' from the Ministry of Education, Culture, Sports, Science and Technology, Japan) for performing the assay for cytotoxicity using a panel of 39 human cell lines. We are

grateful to Ms. M. Fujitake and Dr. K. Minoura of this university for MS and NMR measurements, respectively. This study was supported by a Grant-in-Aid for High Technology Research from the Ministry of Education, Culture, Sports, Science and Technology, Japan.

References and notes

1. Iwamoto, C.; Yamada, T.; Ito, Y.; Minoura, K.; Numata, A. *Tetrahedron* **2001**, *57*, 2997–3004.
2. Yamada, T.; Iritani, M.; Doi, M.; Minoura, K.; Ito, T.; Numata, A. *J. Chem. Soc., Perkin Trans. 1* **2001**, 3046–3053.
3. Yamada, T.; Iritani, M.; Minoura, K.; Numata, A. *J. Antibiot.* **2002**, *55*, 147–154.
4. Yamada, T.; Iritani, M.; Minoura, K.; Kawai, K.; Numata, A. *Org. Biomol. Chem.* **2004**, *2*, 2131–2135.
5. Yamada, T.; Imai, E.; Nakatani, K.; Numata, A.; Tanaka, R. *Tetrahedron Lett.* **2007**, *48*, 6294–6296.
6. Yamada, T.; Iritani, M.; Ohishi, H.; Tanaka, K.; Minoura, K.; Doi, M.; Numata, A. *Org. Biomol. Chem.* **2007**, *5*, 3979–3986 and references cited therein.
7. Yamada, T.; Doi, M.; Shigeta, H.; Muroga, Y.; Hosoe, S.; Numata, A.; Tanaka, R. *Tetrahedron Lett.* **2008**, *49*, 4192–4195.
8. Muroga, Y.; Yamada, T.; Numata, A.; Tanaka, R. *J. Antibiot.* **2008**, *61*, 615–622.
9. Quang, D. N.; Stadler, M.; Fournier, J.; Tomita, A.; Hashimoto, T. *Tetrahedron* **2006**, *62*, 6349–6354.
10. Matsuzaki, K.; Tahara, H.; Inokoshi, J.; Tanaka, H. *J. Antibiot.* **1998**, *51*, 1004–1011.
11. Yoshida, E.; Fujimoto, H.; Yamazaki, M. *Chem. Pharm. Bull.* **1996**, *44*, 284–287.
12. Takahashi, M.; Koyama, K.; Natori, S. *Chem. Pharm. Bull.* **1990**, *38*, 625–628.
13. Toki, S.; Tanaka, T.; Uosaki, Y.; Yoshida, M.; Suzuki, Y.; Kita, K.; Mihara, A.; Ando, K.; Lokker, N. A.; Giese, N. A.; Matsuda, Y. *J. Antibiot.* **1999**, *52*, 235–244.
14. Phomkerd, N.; Kanokmedhakul, S.; Kanokmedhakul, K.; Soyong, K.; Prabpai, S.; Kongsearee, P. *Tetrahedron* **2008**, *64*, 9636–9645.
15. Mathe, F.; Castanet, Y.; Mortreux, A.; Petit, F. *Tetrahedron Lett.* **1991**, *32*, 3989–3992.
16. Whalley, W. B.; Ferguson, G.; Marsh, W.; Restivo, R. *J. Chem. Soc., Perkin Trans. 1* **1976**, 1366–1369.
17. Steyn, P. S.; Vlegaar, R. *J. Chem. Soc., Perkin Trans. 1* **1976**, 204–206.
18. Yamori, T.; Matsunaga, A.; Sato, S.; Yamazaki, K.; Komi, A.; Ishizu, K.; Mita, I.; Edatsugi, H.; Matsuba, Y.; Takezawa, K.; Nakanishi, O.; Kohno, H.; Nakajima, Y.; Komatsu, H.; Andoh, T.; Tsuruo, T. *Cancer Res.* **1999**, *59*, 4042–4049.
19. Yamori, T. *Cancer Chemother. Pharmacol.* **2003**, *52*, S74–S79.